

## Transition temperature and irreversibility line of cobalt-doped single-crystal $\text{YBa}_2\text{Cu}_3\text{O}_{7-\delta}$ : The effect of high-pressure oxygen annealing

R. L. Neiman, J. Giapintzakis, and D. M. Ginsberg

*Department of Physics and Materials Research Laboratory, University of Illinois at Urbana-Champaign,  
1110 West Green Street, Urbana, Illinois 61801*

(Received 15 July 1994)

We have measured the effect of cobalt on the superconducting transition temperature ( $T_c$ ) and the dc irreversibility line (IRL) of single-crystal  $\text{YBa}_2\text{Cu}_3\text{O}_{7-\delta}$  (YBCO).  $T_c$  of a single crystal annealed in flowing oxygen at atmospheric pressure is markedly lower than that of a polycrystalline sample with the same cobalt concentration and annealing pressure. High-pressure oxygen annealing (HPA) increases  $T_c$  to a value comparable to that of a polycrystalline sample. This increase implies that Co-doped YBCO single crystals low-pressure annealed (LPA) in flowing oxygen are not as fully oxygenated as polycrystalline samples. The IRL was found to have two different functional behaviors, one for low concentrations of cobalt and another for high concentrations. By comparison with the Bi-Sr-Ca-Cu-O and Tl-Ba-Ca-Cu-O systems, this change in functional behavior is attributed to a decrease in coupling between Cu-O planes.

### I. INTRODUCTION

$\text{YBa}_2\text{Cu}_3\text{O}_{7-\delta}$  (YBCO) is unusual among the cuprate superconductors, as it has Cu-O chains as well as Cu-O planes. Since cobalt substitutes in the chains at the low concentrations that we use, we have investigated the role of the chains on the superconducting properties of YBCO by systematically changing the concentration of cobalt, a magnetic ion.

### II. BACKGROUND: POLYCRYSTALLINE STUDIES

Neutron-diffraction measurements have shown that cobalt substitutes on the chains<sup>1</sup> at the low concentrations that we use. The cobalt ion has a valence of  $3^+$ , and replaces copper having a valence of  $2^+$ . This change in valence leads to an increase in the oxygen concentration per unit cell.<sup>2</sup> The extra oxygens have been found to occupy the O(5) lattice site (the oxygen site bridging the Cu-O chains).<sup>3</sup> Increasing the cobalt concentration increases the O(4)-to-Cu(2) bond length.<sup>3</sup> In other words, the apical oxygens are pulled away from the planes and toward the chains. This increase in the O(4)-Cu(2) bond length has been linked with the decrease of available carriers on the Cu-O<sub>2</sub> planes.<sup>3</sup>

Cobalt doping has been found to cause a structural symmetry change as well. X-ray powder-diffraction measurements of the *a*- and *b*-axis lattice parameters show an orthorhombic-to-tetragonal phase transition occurring at approximately 2.5% substitution for copper.<sup>4</sup> (We express all doping concentrations in atomic percent.) This phase transition is accompanied by a marked change in the dependence of  $T_c$  on cobalt. While resistive measurements of the transition temperature show a plateau (at approximately  $T_c = 90$  K) for concentrations in the orthorhombic phase,  $T_c$  decreases almost linearly for concentrations in the tetragonal phase.  $T_c$  reaches 0 K at approximately 15% substitution.<sup>4</sup>

### III. EXPERIMENTAL METHOD

The single crystals used in this study were grown by a flux method.<sup>5</sup> In order to grow crystals of *x*% Co-doped YBCO, a molar ratio of Y:Ba:Cu:Co of 1:8:20:10*x* was used. Powders of at least 99.999% pure  $\text{Y}_2\text{O}_3$ ,  $\text{BaCO}_3$ , CuO, and  $\text{Co}_2\text{O}_3$  were ground in an agate mortar and pestle until the powder was homogeneously mixed. The powder was then loosely packed in an yttria-stabilized zirconia crucible and placed in a box furnace. The powders were heated at a rate of  $192^\circ\text{C}/\text{h}$  to  $800^\circ\text{C}$ , then heated at a rate of  $50^\circ\text{C}/\text{h}$  to  $1000^\circ\text{C}$ . The furnace was kept at  $1000^\circ\text{C}$  for 4 h and then slow cooled at a rate of  $4^\circ\text{C}/\text{h}$  to  $865^\circ\text{C}$ , and the crucible was removed. The crucible was broken open, and the crystals were then selected.

After selecting the crystals, we oxygenated them for one hour at  $600^\circ\text{C}$ , and the temperature was reduced to  $410^\circ\text{C}$  for an additional two-week anneal in flowing oxygen to make them superconducting. High-pressure oxygen annealing was performed on some of the crystals in a Morris Research high-pressure furnace<sup>6</sup> for three days at  $410^\circ\text{C}$  and a pressure of 51–53 bar. The crystals that were high-pressure annealed will be referred to as HPA crystals. The crystals ranged in concentration of cobalt from 0% to about 4% substitution, as measured by proton induced x-ray emission (PIXE) and energy dispersive x-ray spectroscopy (EDX).

A low-field Quantum Design superconducting quantum interference device (SQUID) magnetometer<sup>7</sup> was used to measure the crystal's transition temperature and transition width,  $\delta T_c$ . All samples had  $\delta T_c$  less than 3 K in a 1-G field, both before and after high-pressure annealing (see Table I).

The irreversibility line (IRL) was determined in a 5.5-T Quantum Design SQUID magnetometer.<sup>8</sup> In a fixed field, irreversible behavior is indicated when the field-cooled and zero-field-cooled magnetizations are different,

TABLE I. Summary of sample  $T_c$ 's with low-pressure annealing (LPA) and high-pressure annealing (HPA).  $x$  is the cobalt content.

$x$	$T_c$ , K (LPA)	$T_c$ , K (HPA)
0.01	90.7±0.3	
0.02	88.7±1.0	89.7±0.6
0.025	81.2±1.0	86.8±2.0
0.03	76.1±2.5	86.4±2.0
0.04	66.3±1.0	77.1±2.0

because the critical current density  $J_c > 0$ .<sup>9</sup> The highest temperature at which this difference occurs is denoted by  $T_{irr}$ . The plot of  $H$  vs  $T_{irr}$  shows the IRL.

The IRL was measured as follows. The sample was mounted with GE 7031 varnish onto a nylon string, in order to reduce the background signal due to the sample holder. The nylon string was held taut by a nonmagnetic weight, and the sample was mounted with  $H||c$ . The sample scan length was 4.0 cm, in which the field variation was less than  $\pm 0.19\%$ . The temperature tolerance factor was set to 0.001, leading to variations of temperature less than 0.09 K over the entire temperature range. The slew rate was set at 1.00, the initial rate at 0.50, and the acceleration rate at 1.00 in order to slow the movement of the string. In taking the data, three scans were averaged, and 32 points were taken per scan.

#### IV. RESULTS

##### A. Cobalt's effect on $T_c$

When cobalt is substituted for copper in polycrystalline YBCO,  $T_c$  remains approximately constant at 91 K for substitutions of less than 2%. However in single-crystal  $\text{YBa}_2(\text{Cu}_{1-x}\text{Co}_x)_3\text{O}_{7-\delta}$ ,  $T_c$  decreases for cobalt concentrations as small as 1%. While  $T_c$  of the single-crystal samples is lower than that of the comparable polycrystalline samples for all concentrations of cobalt, optical microscope observations show us that a single-crystal undergoes the orthorhombic-to-tetragonal phase transition at approximately the same concentration as that of a polycrystalline sample.

The lower single-crystal transition temperatures suggest that the single crystals might be under oxygenated. To test this, we high-pressure oxygen annealed (HPA) the single crystals and found that  $T_c$  was increased to a value comparable to that found in the polycrystalline samples (see Fig. 1). This increased  $T_c$  is stable; the HPA samples remain unchanged even after storage in a desiccator for 5 months. However, if a HPA sample is reannealed in flowing oxygen for four days, the transition temperature decreases. ( $T_c$  does not, however, completely return to the original pre-HPA value.)

One should note that high-pressure oxygen annealing has an effect on the width of the transition temperature, although in most cases the effect is  $\leq 10\%$  of  $\delta T_c$ . In samples that have sharp transitions before high-pressure annealing, the transition sometimes broadens slightly, as we will discuss; in samples with broad or multisteped tran-

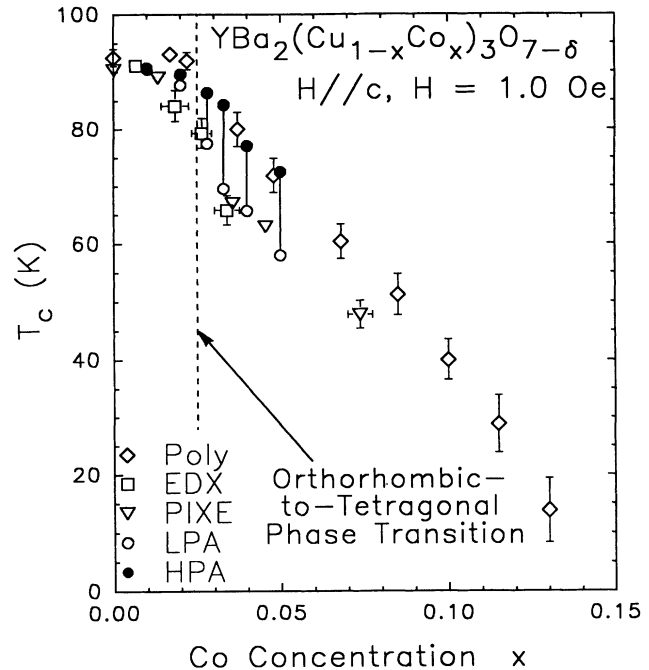


FIG. 1.  $T_c$  vs concentration of cobalt. The Poly data are for polycrystalline samples, from Ref. 4. The energy dispersive x ray (EDX) and proton induced x-ray emission (PIXE) data were measured by using low-pressure annealed (LPA) single crystals. Pairs of data points, connected by a line and labeled LPA and high-pressure annealed (HPA), are for the same sample measured before and after high-pressure annealing.

sitions, the transition usually sharpens, sometimes quite significantly.

##### B. Cobalt's effect on the irreversibility line

Having found that our single crystals grown in flowing  $\text{O}_2$  were not fully oxygenated, we studied the IRL of both low-pressure annealed (LPA) and high-pressure annealed (HPA) crystals. All methods of measuring the IRL have limitations.<sup>10</sup> To minimize the effect of these limitations on comparing our different samples, we chose samples with approximately the same dimensions and masses. The variation from crystal to crystal may be as large as a factor of 5 in the masses. To ensure that our IRL represents a constant value of  $J_c$ , we applied a constant threshold criterion to all of our runs on a given crystal. That is,  $M_{FC}(T_{irr}) = M_{ZFC}(T_{irr}) + \Delta M$ , where  $\Delta M$  is the same for every measurement used to determine  $T_{irr}$ . As has been pointed out,<sup>10,11</sup> this measurement is only a lower limit of the irreversibility line because  $J_c \neq 0$ . The "true" irreversibility line (at  $J_c = 0$ ) would be at higher temperatures than the dc irreversibility line. Since the measurements of each sample were taken at constant values of  $J_c$ , however, we believe the functional behavior of the IRL should be close to that of the "true" IRL.

Before we can investigate the effect of cobalt on the irreversibility line, we must normalize the temperature axis to remove the shift in the IRL caused by the decrease in

$T_c$ . Thus, we plot  $H_{irr}$  versus a normalized temperature  $T/T_c$  in Fig. 2. The IRL shifts to lower fields and temperature on doping with cobalt. Two distinct functional forms are seen: one for samples with low concentrations (LC) of cobalt ( $x \leq 0.025$ ) and one for samples with high concentrations (HC) of cobalt ( $x \geq 0.03$ ). The LC samples obey the functional power law given by the published data on undoped YBCO and zinc-doped YBCO polycrystalline samples:<sup>12</sup>

$$H_{irr} = H_0(1 - T_{irr}/T_c)^n, \quad (1)$$

where  $n \cong 3/2$ . Plotting  $\ln(H_{irr})$  vs  $\ln(1 - T_{irr}/T_c)$  gives a straight line with slope  $n$ , as shown in Fig. 3. The HC samples do not obey the functional power law given above. In order to show qualitatively that the HC samples are different from the LC samples, we fitted  $\ln(H_{irr})$  vs  $\ln(1 - T_{irr}/T_c)$  with a second-order polynomial. The fitting parameters are listed in Table II. The HC samples have a significantly larger quadratic term in their fitting ( $a_2 \cong 0.7$ ) than do the LC samples ( $a_2 \cong 0.06$ ). For the LC samples, we used a linear fit for  $\ln(H_{irr})$  vs  $\ln(1 - T_{irr}/T_c)$  in order to determine the value of  $n$ . We found that  $n = 1.1$  for the 1% substituted sample,  $n = 1.3$  for the 2% substituted sample, and  $n = 1.4$  for the 2.5% substituted sample. These values are approximately the expected value of  $n = 1.5$  (see Table III).

As discussed earlier, LPA cobalt-doped single crystals are under oxygenated. Therefore, high-pressure annealing was performed on some samples and the effect on the IRL was measured (see Fig. 4). The IRL of the LC samples did not show much of a change, except possibly a slight shift to lower temperatures for the higher fields.

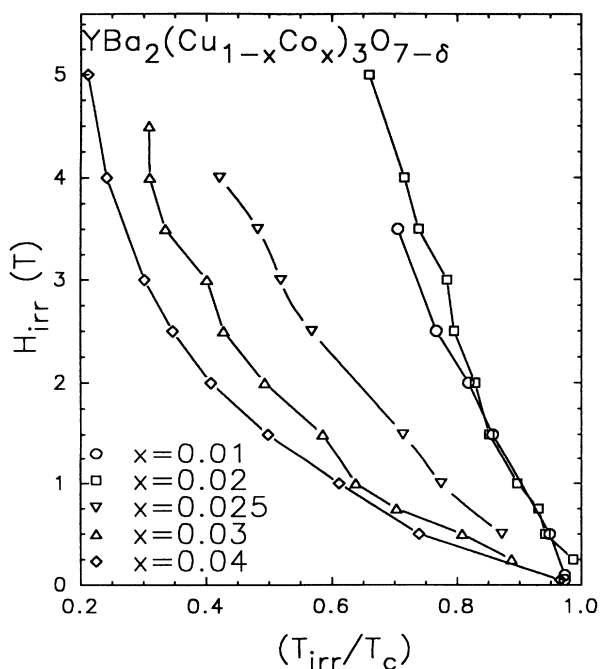


FIG. 2.  $H_{irr}$  vs normalized temperature. The temperature is normalized to separate the effect of cobalt on the irreversibility line from its effect on  $T_c$ .

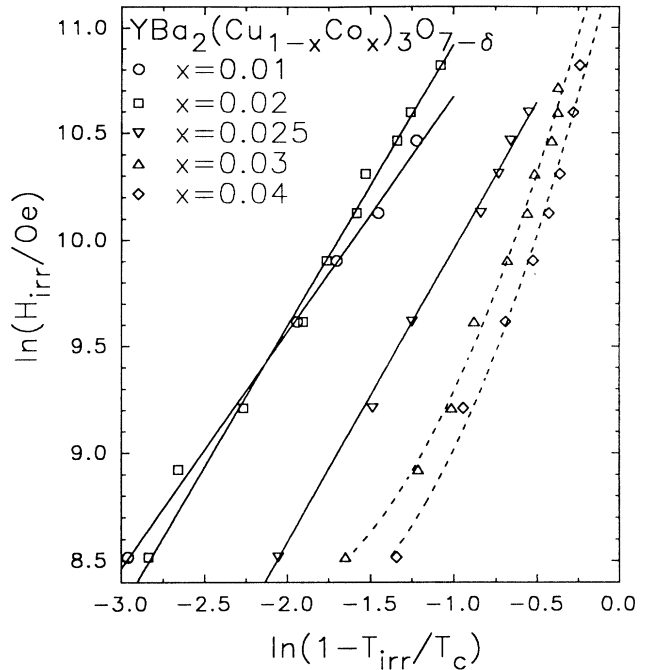


FIG. 3.  $\ln(H_{irr})$  vs  $\ln(1 - T_{irr}/T_c)$ . A linear fit is drawn for the 1%, 2%, and 2.5% samples, while a quadratic fit is plotted for the 3% and 4% samples. The fitting coefficients are listed in Tables II and III.

(However, this shift to lower temperatures may be sample dependent.) The IRL of the HC samples showed an increase to higher temperatures, but again the functional form remained unchanged. (The 3% sample was run both before and after HPA, so we were probing the same value of  $J_c$  before and after HPA.)

## V. DISCUSSION

Unlike polycrystalline cobalt-doped YBCO, single-crystal YBCO is not as fully oxygenated at atmospheric pressure as at high pressures. The reduced oxygen content produced by low-pressure annealing was indicated by the low  $T_c$ 's of the single crystals, when compared to polycrystalline data. We verified this by performing HPA on single crystals at a variety of doping concentrations and measuring  $T_c$ . The HPA crystals gave results comparable to those for polycrystalline samples. We believe this oxygenation problem results from two effects. In the single crystals, the surface area/volume ratio was

TABLE II. Polynomial fit of  $\ln(H_{irr})$  vs  $\ln(1 - T_{irr}/T_c)$ . The fit is  $z = a_0 + a_1 y + a_2 y^2$ , where  $z = \ln(H_{irr})$  and  $y = \ln(1 - T_{irr}/T_c)$ .

$x$	$a_0$	$a_1$	$a_2$
0.01	12.0	1.29	0.045
0.02	12.4	1.53	0.053
0.025	11.4	1.53	0.062
0.03	11.7	3.12	0.720
0.04	11.4	3.19	0.789

TABLE III. Linear fit of  $\ln(H_{irr})$  vs  $\ln(1-T_{irr}/T_c)$ . The fit is  $z = a_0 + a_1 y$ , where  $z = \ln(H_{irr})$  and  $y = \ln(1-T_{irr}/T_c)$ .

$x$	$a_0$	$a_1$
0.01	11.8	1.10
0.02	12.2	1.32
0.025	11.3	1.37

smaller than that of polycrystalline samples. Because of the increased valence of the cobalt, additional oxygen is required, so the conditions to oxygenate the samples may be different from undoped YBCO. Apparently this makes it difficult to fully oxygenate the single-crystal cobalt-doped YBCO in flowing atmospheric-pressure oxygen.

The explanation of the effect of HP on the  $\delta T_c$  is not so straightforward. Naively, one would expect the transition temperature to be sharpened by increasing oxygen because we could be increasing the homogeneity of the oxygen distribution. For most poor quality samples (having very broad  $T_c$ 's), HPA does indeed sharpen the transition width. However, for high quality samples, which show sharp transitions before HPA, the transition can broaden slightly. Since the transition can broaden, we clearly do not have a complete picture of the effects of HPA.

The IRL measurements shed some light on the role of the chains in YBCO. If one compares cobalt-doped YBCO samples with oxygen-reduced samples, it becomes apparent that the cobalt is not having the same impact on

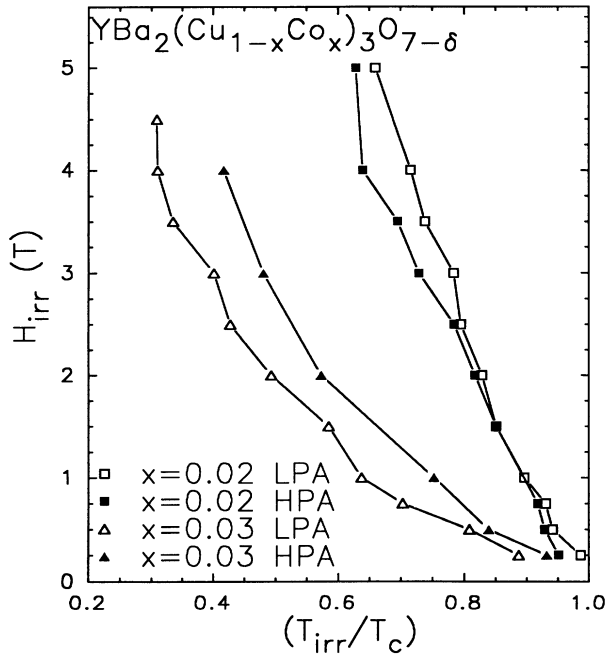


FIG. 4.  $H_{irr}$  vs normalized temperature. The plot shows the effect of high-pressure oxygen annealing (HPA) on 2% and 3% samples. The 2% samples are representative of low concentration (LC) samples, while the 3% sample is representative of high concentration (HC) samples.

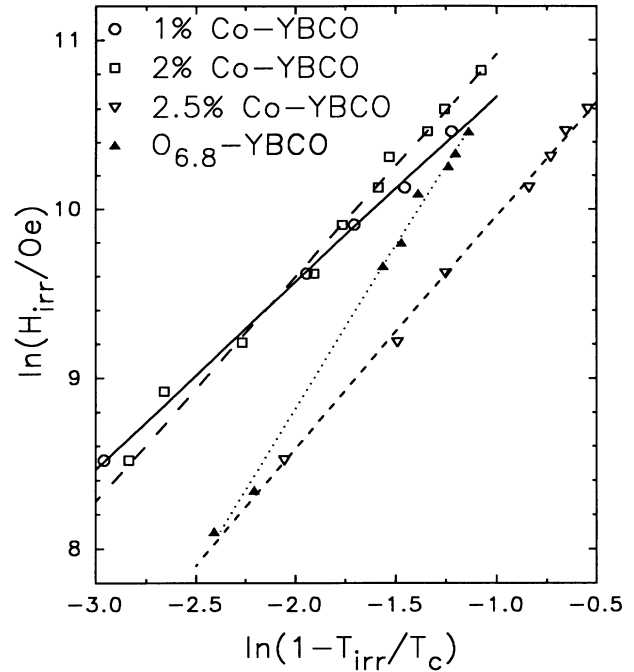


FIG. 5.  $\ln(H_{irr})$  vs  $\ln(1-T_{irr}/T_c)$  for LC Co-doped and oxygen-reduced YBCO samples. The oxygen-reduced data are from Ref. 13. The oxygen-reduced sample has the same functional behavior as the undoped, fully oxygenated YBCO samples, implying that the reduction of oxygen is not leading to the change in functional behavior in the cobalt-doped samples.

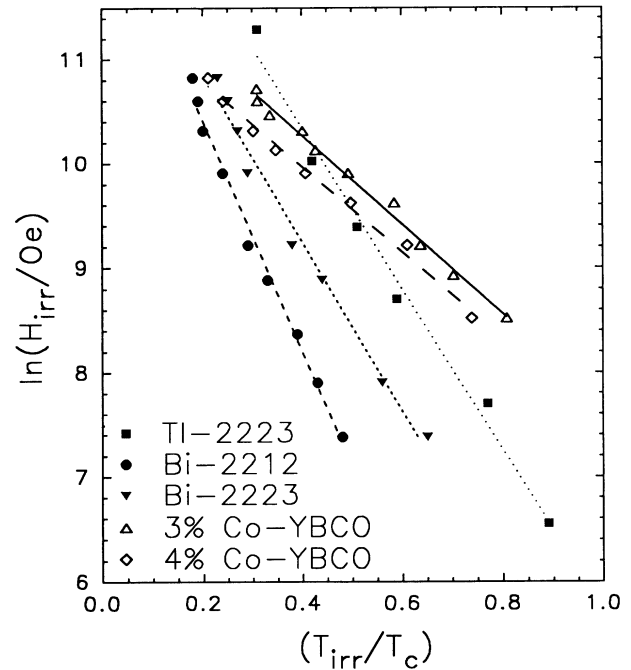


FIG. 6.  $\ln(H_{irr})$  vs  $(T_{irr}/T_c)$  for HC Co-doped YBCO, Bi-2212, Bi-2223, and Tl-2223 samples. The Bi-2212 and Bi-2223 data are from Ref. 14. The Tl-2223 data are from Ref. 15. The HC Co-doped YBCO samples have the same functional behavior as the Bi-2212, Bi-2223, and Tl-2223 samples, implying that the cobalt is decreasing the coupling between the Cu-O planes.

the IRL as the oxygen. Even for crystals with oxygen content of 6.8,<sup>13</sup> the IRL still obeys Eq. (1) (see Fig. 5). Therefore we conclude that the reduced oxygen state of the LPA cobalt-doped YBCO samples cannot explain the change in functional form for HC cobalt-doped YBCO samples.

However, if one examines Bi-2212, Bi-2223,<sup>14</sup> and Tl-2223,<sup>15</sup> one sees another functional behavior, where  $\ln(H_{\text{irr}})$  vs  $(T_{\text{irr}}/T_c)$  is linear. When one plots the HC cobalt-doped YBCO samples in the same manner, one sees a similar behavior, but the slopes for the Co-doped YBCO samples are smaller (see Fig. 6). As the Bi-Sr-Ca-Cu-O (BSCCO) and Tl-Ba-Ca-Cu-O (TBCCO) systems are known to be much more anisotropic than the YBCO system, it appears that by increasing the cobalt in the sample, we are accomplishing the same effect as decreasing the coupling of the Cu-O planes. The anisotropy may therefore be associated with a deviation from the expected functional form for the IRL. Alternatively, since the change in functional form occurs between 2.5 and 3% substitution, the effect may be associated with the orthorhombic-to-tetragonal phase transition, which occurs in that range.

## VI. CONCLUSIONS

We have measured  $T_c$  and the IRL of cobalt-doped single-crystal YBCO samples. We find that cobalt-doped samples are under oxygenated when annealed under standard annealing methods, but can be more fully oxygenated by high-pressure oxygen annealing. We also find that the irreversibility line of cobalt-doped YBCO changes functional form at approximately 2.5–3% cobalt substitution, where the orthorhombic-to-tetragonal phase transition occurs. By comparison with the BSCCO and TBCCO systems, the data seem to imply that an increase in cobalt content decreases the ability of the chains to couple the Cu-O planes.

## ACKNOWLEDGMENTS

This work was supported by National Science Foundation Grant No. DMR 89-20538 (R.L.N.), and by NSF Grant No. DMR 91-20000 through the Science and Technology Center for Superconductivity (J.G. and D.M.G.).

<sup>1</sup>J. F. Bringley, T.-M. Chen, B. A. Averill, K. M. Wong, and S. J. Poon, *Phys. Rev. B* **38**, 2432 (1988).

<sup>2</sup>Ryozo Aoki, Singo Takahashi, Hironaru Murakami, Tetsuro Nakamura, Takahiro Nakamura, Yoshiki Takagi, and Ruixing Liang, *Physica C* **156**, 405 (1988).

<sup>3</sup>P. F. Miceli, J. M. Tarascon, L. H. Greene, P. Barboux, F. J. Rotella, and J. D. Jorgensen, *Phys. Rev. B* **37**, 5932 (1988).

<sup>4</sup>Izumi Sankawa, Makoto Sato, and Tsuneo Konaka, *Jpn. J. Appl. Phys.* **27**, L28 (1988).

<sup>5</sup>J. P. Rice, B. G. Pazol, D. M. Ginsberg, T. J. Moran, and M. B. Weissman, *J. Low Temp. Phys.* **72**, 345 (1988).

<sup>6</sup>High Pressure Oxygen System Model HPS 3210, Morris Research Inc., 1918 University Ave., Berkeley, CA 94704.

<sup>7</sup>Quantum Design SQUID Model MPMS<sub>2</sub>, Quantum Design, 11578 Sorrento Valley Road, Suite 30, San Diego, CA 92121.

<sup>8</sup>Quantum Design, SQUID Model MPMS.

<sup>9</sup>C. P. Bean, *Phys. Rev. Lett.* **8**, 250 (1962); *Rev. Mod. Phys.* **36**, 31 (1964).

<sup>10</sup>A. K. Grover, S. Ramakrishnan, Ravi Kumar, P. L. Paulose, G. Chandra, S. K. Malik, and P. Chaddah, *Physica C* **192**, 372 (1992).

<sup>11</sup>J. Giapintzakis, R. L. Neiman, D. M. Ginsberg, and M. A. Kirk, *Phys. Rev. B* **50**, 16001 (1994).

<sup>12</sup>D. N. Zheng, J. D. Johnson, and A. M. Campbell, *Supercond. Sci. Tech.* **5**, S495 (1992).

<sup>13</sup>J. G. Ossandon, J. R. Thompson, D. K. Christen, B. C. Sales, H. R. Kerchner, J. O. Thomson, Y. R. Sun, K. W. Lay, and J. E. Tkaczyk, *Phys. Rev. B* **45**, 12534 (1992).

<sup>14</sup>M. Suenaga, D. O. Welch, and R. Budhani, *Supercond. Sci. Tech.* **5**, S1 (1992).

<sup>15</sup>W. Y. Liang, *Physica C* **209**, 237 (1993).